ATLAS Internal Note
LARG-No-035
Date 29 FEV 96

NEW NOISE FIGURES FOR THE ATLAS E.M. CALORIMETER

C. de La Taille
Laboratoire de l'Accélérateur Linéaire (LAL), 91 405 Orsay, FRANCE

1 Introduction

This short note summarizes the latest noise figures in MeV for the ATLAS electromagnetic calorimeters with GaAs [1] or ØT [2] preamplifiers. They are obtained from ENI[1] measurements on preamplifiers in the full ATLAS configuration[2] [3] as a function of the measured overall peaking time to the triangle $t_p(\Delta)$ [*from D. Camin and Y. Jacquier*]. The noise is then fitted according to the equation[3] :

$$ENI^2 = \frac{A}{t_p^5(\Delta)} + \frac{B}{t_p^3(\Delta)} + \frac{C}{t_p(\Delta)} \tag{2}$$

[1]ENI=Equivalent Noise Current : with current sensitive preamplifiers, the electronic noise is referred to the input as a current (ENI) (similarly to ENC for the charge preamplifiers) and is usually expressed in nA *rms*.

[2]correct detector capacitance, cable length and dynamic range

[3]As shown in Ref. [6], the noise can be written :

$$ENI^2 = 5060\,\frac{e_n^2 C_d^2}{t_p^3(\Delta)} + 770\,\frac{i_n^2}{t_p(\Delta)} \tag{1}$$

in the units of nA *rms*, nV/$\sqrt{\text{Hz}}$, pF, ns and pA/$\sqrt{\text{Hz}}$. This equation is independent of the shaper and of the preamp risetime when the peaking time 5-100% is used. For cold current preamplifiers, the first term corresponds to the series noise and the second term to the parallel noise, dominated by the feedback and calibration resistors. For ØT preamps, the same slopes exist, but cannot be attributed to series or parallel noise as they depend on the cable length compared to the shaping time. In Eq.(2) the first term in A/t_p^5 is added empirically to obtain a good fit at fast shaping and may come from an increasing shaper noise contribution due to second pole in the preamp [4].

The coefficients A, B and C are obtained for various detector capacitance values (corresponding to various rapidities) and are interpolated over the whole rapidity range to obtain a function of η (or $\sin\theta$).

The conversion into MeV is achieved from the measured nA/MeV ratio obtained in RD3, scaled by the new sampling fractions[4] in ATLAS for the Barrel and the End-Cap [*from J. Colas and E. Monnier*].

This provides a noise estimate as a function of $t_p(\Delta)$ and $\sin\theta$. Including the latest pileup noise figures (taking into account the empty bunches) [*from V. Tisserand*] yields the optimum shaping and noise figure at any rapidity. Examples are given for a 3×7 cluster (without presampler[5]) in the Barrel ($\eta = 0$ and $\eta = 1.4$) and in the middle of the End-Cap ($\eta = 2$).

2 Barrel Calorimeter

2.1 Conversion nA/MeV

On the RD3 calorimeter, the conversion factor I_0/E has been measured to be 2.33 nA/MeV in a nonnet and 2.57 nA/MeV in a large window [4], in fair agreement with calculations [6]. In ATLAS, the sampling fraction is larger as the lead is thinner (cf. Table 1) and the liquid argon gap is larger, which leads to a larger deposited charge. However, the drift time is also longer, especially when keeping the same high voltage[6] (V=2 kV) (t_{dr} = 455 ns compared to 400 ns) which reduces in proportion the initial triangular current I_0 [7].

Thus, scaling with the sampling fractions calculated in Table 1 and drift times yields a conversion factor[7] :

$$\frac{I_0}{E} = 2.57 * \frac{0.247}{0.204} * \frac{400}{455} = 2.74 \text{ nA/MeV} \qquad 0 < \eta < 0.8 \quad (48^o < \theta < 90^o) \qquad (4)$$

$$\frac{I_0}{E} = 2.57 * \frac{0.278}{0.204} * \frac{400}{455} = 3.08 \text{ nA/MeV} \qquad 0.8 < \eta < 1.4 \quad (28^o < \theta < 48^o) \qquad (5)$$

[4] including the change in lead thickness at $\eta = 0.8$

[5] The presampler has not been included (it is treated in Ref. [5]) but all the front strips in the cluster are taken which probably gives similar performance as an optimized cluster with presampler.

[6] In RD3, the drift time has been measured $t_{dr} = 400$ ns with 1.9 mm Argon gap and 2 kV high voltage [7]. In ATLAS, raising the gap to 2.1 mm increases the drift time by 10 % but also lowers the electric field by 10 %. Using the parametrization for drift time versus electric field given in Ref [7] gives :

$$t_{dr} = \frac{400\,g}{1.9} \frac{1}{0.274\left(\frac{1.9U}{g}\right)^{0.222} - 0.475} \qquad (3)$$

t_{dr} in ns, g gap size in mm and U high voltage in V.

[7] the e/μ ratio is included in the 2.57 nA/MeV measured on RD3. Taking $W_i = 24$ eV leads to $e/\mu = 0.76$, in good agreement with the values given by Montecarlo simulations [8].

2.2 Noise with ∅T 50 Ω in the Front sampling

The Front sampling is 4.5 X_0 deep (tapered) and segmented in $\Delta\eta \times \Delta\phi = 0.0031 \times 0.1$. The detector capacitance[8] is around 150 pF and ∅T preamps [2] are used with a 50 Ω cable varying from 6 to 2 meters along η. In this configuration, ENI has been measured (cf. Fig.3) and can be fitted as (cf. Table 3) :

$$ENI_F^2 = \frac{0.5\,10^8}{t_p^3(\Delta)} + \frac{6\,10^4}{t_p(\Delta)} \qquad \forall\theta \tag{6}$$

where ENI is in nA *rms* and $t_p(\Delta)$ is the peaking time 5-100% to the triangle in ns. For example, at $t_p(\Delta) = 40$ ns, $ENI_F = 48$ nA. It is almost independent of θ as the detector capacitance does not vary (because of the tapering) and the noise is little affected by the cable length at small C_d.

ENI can be converted into energy, using Eq.(4) and (5) :

$$ENE_F = \frac{ENI_F}{2.74}\,\frac{\text{MeV}}{\text{nA}} \qquad 48^o < \theta < 90^o \tag{7}$$

$$ENE_F = \frac{ENI_F}{3.08}\,\frac{\text{MeV}}{\text{nA}} \qquad 28^o < \theta < 48^o \tag{8}$$

2.3 Noise with GaAs in the Middle and Back samplings

The Middle sampling is 13 $X_0/\sin\theta$ deep[9] [3], segmented in 0.025 x 0.025 and the Back sampling is 7.5 $X_0/\sin\theta$, 0.025 $\times$ 0.05, which leads to a similar detector capacitance. It increases with rapidity as the cell length scales as $1/\sin\theta$. The maximum current also roughly scales with $1/\sin\theta$ and is around 5 mA in the middle sampling at $\eta = 0$[10]. In the Back sampling, the maximum current is less, but this does not change significantly the preamp noise and the calculations have been performed using the same figures in Middle and Back.

$$C_d = \frac{1\,\text{nF}}{\sin\theta} \quad \Rightarrow \quad 1\,\text{nF} < \text{C}_\text{d} < 2.2\,\text{nF} \qquad I_0 < \frac{5\,\text{mA}}{\sin\theta} \tag{9}$$

Current sensitive GaAs preamps [1] would be installed right onto the electrodes to amplify the detector current and achieve minimum white and coherent noise. The noise has been measured on bench at LAr temperature in three configurations : $\eta = 0$, 1 and 1.4

[8] This is only the capacitance to ground, there is a crosstalk capacitance to the neighbours of similar value, which induces partially anti-correlated noise as a function of the cable length [9]. The net result in a cluster should therefore be checked.

[9] In case of a tapered Middle sampling [10], Eq.(10) still holds, replacing $\sin\theta$ by 1 nF/C_d in the first two terms (but not in the third one). For example, if it is tapered at 18 X_0, C_d = 1.5 nF, which is equivalent to using $\sin\theta = 0.75$.

[10] The maximum energy in a cell at $\eta = 0$ is 1.5 TeV [3] with 2.74 mA/TeV giving 4.1 mA. At $\eta = 1.4$, kinematic limits keep the maximum energy below 2.5 TeV, but the current is larger with 3.08 mA/TeV, giving 7.9 mA.

corresponding to C_d = 1, 1.5 and 2.2 nF (cf. Fig.1), with the feedback network also scaled in accordance to accomodate the larger current[11]. The preamplifier used for the measurements exhibits a noise spectral density $e_n = 0.24$ nV/$\sqrt{\text{Hz}}$, which corresponds to the best figures so far obtained with these preamps[12]. The protection for high voltage sparking was not installed[13]. From the fit coefficients given in Table 3, the noise can be written :

$$ENI^2_{MB} = \frac{0.1\,10^{12}}{\sin^4\theta\, t_p^5(\Delta)} + \frac{2.4\,10^8}{\sin^2\theta\, t_p^3(\Delta)} + \frac{3\,10^4}{\sin\theta\, t_p(\Delta)} \tag{10}$$

ENI in nA *rms* and $t_p(\Delta)$ in ns. The dependence with $\sin\theta$ is determined empirically[14]. ENI can be converted into energy using Eq.(4) and (5) as in Eq.(7) and (8).

2.4 Noise with ∅T 25 Ω in the Middle and Back samplings

For large detector capacitance ($C_d > 1$ nF), a 25 Ω cable gives better results than a 50 Ω one, as can be seen comparing Fig.2 and Fig.3. In this section of the barrel, the cable would be typically from 1.5 to 5 meters long[15]. Similarly to GaAs preamps, the noise has been measured in three configurations : C_d = 1, 1.5 and 2.2 nF and the corresponding cable lengths[16] (cf. Fig.2). There was also no protection against high voltage sparkings[17]. From the fit coefficients given in Table 3, the noise can be written :

$$ENI^2_{MB} = \frac{0.7\,10^{12}}{\sin^2\theta\, t_p^5(\Delta)} + \frac{4\,10^8}{\sin^2\theta\, t_p^3(\Delta)} + \frac{20\,10^4}{t_p(\Delta)} \tag{11}$$

ENI in nA *rms* and $t_p(\Delta)$ in ns. Again, the dependance with $\sin\theta$ is determined empirically and slightly deteriorates towards 30°. ENI can be converted into energy as in Eq.(7) and (8).

[11] The maximum signal increases as $1/\sin\theta$ in the Barrel. In ATLAS, both feedback and calibration resistors would scale with $\sin\theta$ in order to produce an output signal proportionnal to E_T.

[12] In Refs. [1], [4] and [3], the noise is comprised between 0.2 and 0.4 nV/$\sqrt{\text{Hz}}$, with an average value of 0.3 nV/$\sqrt{\text{Hz}}$ (at 60 mW power dissipation). Part of this dispersion was traced to internal second stage noise, which should be improved in the forcoming version.

[13] It consists of 2 zener diodes and an inductor, which increase the input capacitance by 150 pF and the series noise correspondingly.

[14] The series noise term B is proportionnal to C_d^2 (cf. Eq.(1)) which scales as $1/\sin^2\theta$. The parallel noise term C is proportionnal to the feedback and calibration resistors which scale as $1/\sin\theta$. The shaper noise term A should be proportionnal to C_d^2 [4] but seems here to scale as C_d^4 (cf. Table 3).

[15] 1.5 m is for the end of the barrel, just beneath the feedthrus. It includes 40 cm inside the feedthrus and up to 50 cm outside to the electronic boxes, in case the ∅T does not fit right on the feedthru.

[16] The measurements have been performed at room temperature with 2 LEMO cables in parallel to obtain 25 Ω. When a more ATLAS like cable is used (kapton 1.2 mm) at liquid argon temperature, the noise improves by up to 40 % [12] as both signal attenuation and skin effect thermal noise are reduced.

[17] The HV protection is obtained with 4 or 6 1N4148 diodes and an inductor, which add around 10 pF giving negligible effect on noise performance.

2.5 Optimum noise

Summing quadratically the pileup noise and the total electronic noise in a 3 $\times$ 7 cluster leads to an optimum shaping time to achieve the lowest noise at a given luminosity [6]. The electronic noise in a 3 $\times$ 7 cluster is obtained by summing 48 cells in the Front[18] (equipped with $\emptyset$T 50 Ω) using Eq.(6) and 21+12 cells in Middle and Back, using Eq.(10) or (11) and converting into MeV with Eq.(4) and (5). The pileup noise in a 3 $\times$ 7 cluster is taken from Ref. [11], corrected by $\sqrt{4/3}$ to take into account the empty bunch every four :

$$\sigma^2_{pu} = \frac{3330}{\sin^2\theta} * t_p(\Delta) \quad \text{MeV}^2 \qquad \text{at} \quad \mathcal{L} = 10^{34} \tag{12}$$

It corresponds to 365 MeV at 40 ns and $\eta = 0$.

The results are shown in Fig.5 with GaAs preamps and Fig.6 with $\emptyset$T. The optimum peaking time at $\mathcal{L} = 10^{33}$ and 10^{34} as well as the various noise figures at this shaping are summarized in Table 4. At maximum luminosity, the total noise (electronics $\oplus$ pileup amounts to : σ_{tot} = 410 MeV at $t_p(\Delta) \approx$ 35 ns with GaAs and σ_{tot} = 460 MeV at $t_p(\Delta) \approx$ 45 ns with $\emptyset$T. In the second half of the barrel ($\eta = 1$), the optimum noise has also been computed using the actual measurements from Table 3 and are shown in Table 5, Fig.7 and 8. At maximum luminosity, σ_{tot} = 614 MeV with GaAs and 670 MeV with $\emptyset$T, correspnding to 398 and 434 MeV in transverse energy.

3 End-Cap calorimeter

3.1 Conversion nA/MeV

In the End-Cap [13], the lead thickness is kept constant (1.7 mm in the outer wheel and 2.2 mm in the inner wheel) while the gap decreases, which changes the sampling fraction with rapidity (cf Table 2). However, the high voltage is also varied (from 2500 to 500 V in the outer wheel and 2500 to 1000 V in the inner wheel), to compensate largely this signal change, so that the ratio I_0/E can be taken constant as a first approximation[19] :

$$\frac{I_0}{E} = 2.57 * \frac{0.280}{0.204} * \frac{400}{570} = 2.48 \text{ nA/MeV} \qquad 1.45 < \eta < 2.45 \quad (10^o < \theta < 27^o) \tag{13}$$

$$\frac{I_0}{E} = 2.57 * \frac{0.241}{0.204} * \frac{400}{590} = 2.06 \text{ nA/MeV} \qquad 2.5 < \eta < 3.2 \quad (5^o < \theta < 10^o) \tag{14}$$

[18] this large area may be pessimistic, but can be balanced with the omission of the presampler.

[19] In the outer wheel, the calculation is done at $\eta = 1.5$ with a 2.6 mm gap and 2.4 kV high voltage, using Eq.(3). In the inner wheel, $\eta = 2.5$ with 2.7 mm gap and 2.5 kV.

3.2 Noise with ∅T 50 Ω in the Front sampling

The Front sampling is very similar to the barrel for the outer wheel, whereas the inner wheel has no fine segmentation. As shown in Fig.4, the detector capacitance is also here around 150 pF. The same equation giving ENI can be used there :

$$ENI_F^2 = \frac{0.5\,10^8}{t_p^3(\Delta)} + \frac{6\,10^4}{t_p(\Delta)} \qquad \forall\theta \tag{15}$$

ENI is converted into energy, using Eq.(13) and Eq.(14).

3.3 Noise with ∅T 50 Ω in the Middle and Back samplings

As can be seen in Fig.4, The middle and Back samplings have a similar capacitance which varies largely with η, but remains always smaller than 1 nF. In that case, the 50 Ω cable gives the best results and would be typically from 4 to 6 meters long. Due to kinematic limits, the maximum current is roughly constant : $I_0 < 6$ mA, corresponding to 2.5 TeV. The detector capacitance can be nicely fitted as [13] :

$$C_d = \alpha + \beta \tan^2\theta \qquad\qquad 400\,\mathrm{pF} < \mathrm{C_d} < 1000\,\mathrm{pF}$$

in which α and β are given in Fig.4.

From the fit coefficients given in Table 3, the noise can be written :

$$ENI_{MB}^2 = \frac{10^3\,C_d^3}{t_p^5(\Delta)} + \frac{12\,10^2\,C_d^2}{t_p^3(\Delta)} + \frac{7\,10^4}{t_p(\Delta)} \tag{16}$$

In which ENI is in nA, C_d in pF and $t_p(\Delta)$ in ns. It should be noticed that the noise now decreases with rapidity, as oppposed to the barrel, as the detector capacitance goes down.

3.4 Optimum noise

In the End-Cap, the noise is now decreasing with rapidity, whereas the pileup is still increasing as $1/\sin\theta$. This advocates for shorter and shorter peaking times to minimize the pileup contribution, although the optimum peaking time will probably be determined by the fastest reasonnable value achievable. For timing and calibration accuracy[20] this leads to a peaking time $t_p(\Delta) = 30$ ns. For example, the total noise is shown in Fig.9 in the middle of the outer wheel ($\eta = 2$), and leads at 30 ns, to a total noise of 1250 MeV, corresponding to 360 MeV in transverse energy.

[20] as shown in Ref. [14], the timing accuracy obtained with multiple samples degrades very quickly when there are not enough samples on the waveform. With a 40 MHz digitization frequency, this corresponds to a peaking time of $t_p(\Delta) = 30$ ns. Moreover, at very short peaking times, the inductance effects which can affect differently the calibration and the detector signal start to show up.

4 Conclusion

The more accurate measurements in the ATLAS like configuration have not changed drastically the figures obtained previously [15]. At maximum luminosity, the optimum noise is around 410 MeV at $t_p(\Delta) = 35$ ns with the best GaAs preamplifiers in the Middle and Back sections and around 460 MeV at 45 ns with ØT 25 Ω preamps. In the End-Cap, the optimum shaping is limited by the fastest reasonnable value compatible with the digitization speed, leading to $t_p(\Delta) = 30$ ns. The noise is therefore dominated by the pileup noise at high luminosity, whereas the electronics noise is comparable (or lower) to the barrel figures. It should be emphasized that the electronic noise figures come from few measurements and should therefore be confirmed with more statistics or used with error bars, typically ± 20%.

References

[1] D.V. Camin, N Fedyakin : ATLAS Note LArG-No-011

[2] R.L. Chase et al. : NIM A343 (1994) 598-605

[3] ATLAS Technical Proposal CERN/LHCC/94-43

[4] J. Colas : Note in preparation

[5] E. Albertson, J. Collot : ATLAS Note LArG-No-023

[6] R.L. Chase et al. : ATLAS Note LArG-No-010

[7] C. de La Taille, L. Serin : ATLAS Note Larg-No-029

[8] P. Petroff : private communication

[9] Y. Jacquier et al. : ATLAS Note Larg-No-031

[10] M. Seman : LArG Simulation meeting 30 jan 96

[11] L. serin, V. Tisserand : ATLAS Note CAL-No-073

[12] Y. Jacquier : LArG electronics meeting 31 jan 96

[13] O. Martin, E Monnier, S. Tisserant : Note in preparation

[14] I. Wingerter-Seez : ATLAS Note LArG-No-19

[15] C. de La Taille : LArG electronics meeting 17 may 95

Material	RD3		ATLAS	$0 < \eta < 0.8$	ATLAS	$0.8 < \eta < 1.4$
Lead	1.8 mm	2.309 MeV	1.5 mm	1.924 MeV	1.1 mm	1.411 MeV
Stainless	0.4 mm	0.466 MeV	0.4 mm	0.466 MeV	0.4 mm	0.466 MeV
Prepreg	0.4 mm	0.127 MeV	0.26 mm	0.087 MeV	0.66 mm	0.210 MeV
Copper	0.1 mm	0.129 MeV	0.1 mm	0.129 MeV	0.1 mm	0.129 MeV
Kapton	0.3 mm	0.095 MeV	0.3 mm	0.095 MeV	0.3 mm	0.095 MeV
LAr	3.8 mm	0.803 MeV	4.2 mm	0.888 MeV	4.2 mm	0.888 MeV
Total	6.8 mm	3.929 MeV	6.8 mm	3.585 MeV	6.8 mm	3.199 MeV
η_s		0.2044		0.247		0.278

Table 1: *Sampling fractions η_s in RD3 and in ATLAS Barrel*

Material	Outer Wheel	$1.4 < \eta < 2.5$	Inner Wheel	$2.5 < \eta < 3.2$
Lead	1.7 mm	2.180 MeV	2.2 mm	2.821 MeV
Stainless	0.4 mm	0.466 MeV	0.4 mm	0.466 MeV
Prepreg	0.26 mm	0.087 MeV	0.26 mm	0.087 MeV
Copper	0.1 mm	0.129 MeV	0.1 mm	0.129 MeV
Kapton	0.3 mm	0.095 MeV	0.3 mm	0.095 MeV
LAr	5.6 $\rightarrow$ 2 mm	1.182 $\rightarrow$ 0.423 MeV	5.4 $\rightarrow$ 3.2 mm	1.142 $\rightarrow$ 0.675 MeV
Total	8.2 $\rightarrow$ 4.6 mm	4.139 $\rightarrow$ 3.380 MeV	8.5 $\rightarrow$ 6.5 mm	4.740 $\rightarrow$ 4.273 MeV
η_s		0.286 $\rightarrow$ 0.125		0.241 $\rightarrow$ 0.158

Table 2: *Sampling fractions η_s in ATLAS End-Cap*

Configuration	C_d	A	B	C
AsGa	1 nF	$0.1\,10^{12}$	$2.4\,10^8$	$3\,10^4$
	1.5 nF	$0.5\,10^{12}$	$6\,10^8$	$4.5\,10^4$
	2.2 nF	$2\,10^{12}$	$11\,10^8$	$6.5\,10^4$
ØT 25 Ω	1 nF	$0.7\,10^{12}$	$4\,10^8$	$20\,10^4$
	1.5 nF	$1.4\,10^{12}$	$10\,10^8$	$20\,10^4$
	2.2 nF	$2.8\,10^{12}$	$28\,10^8$	$20\,10^4$
ØT 50 Ω	150 pF	-	$0.5\,10^8$	$6\,10^4$
	390 pF	$0.06\,10^{12}$	$2\,10^8$	$7\,10^4$
	1 nF	10^{12}	$12\,10^8$	$7\,10^4$

Table 3: *Fit coefficients of ENI (nA rms) as a function of $t_p(\Delta)$ (ns) given by Eq.(2) for the various preamplifiers configurations and detector capacitances described in Fig.1, 2 and 3.*

Preamp	$\mathcal{L}$	$t_p^{opt}(\Delta)$	σ_{tot}	σ_{pu}	ENE_{tot}	ENE_F	ENE_{MB}
AsGa	10^{33}	68 ns	187 MeV	150 MeV	111 MeV	82 MeV	75 MeV
AsGa	10^{34}	37 ns	413 MeV	351 MeV	217 MeV	129 MeV	175 MeV
$\emptyset$T 25 Ω	10^{33}	80 ns	216 MeV	163 MeV	143 MeV	74 MeV	124 MeV
$\emptyset$T 25 Ω	10^{34}	46 ns	460 MeV	391 MeV	244 MeV	108 MeV	219 MeV

Table 4: *Optimum peaking time and noise values at $\eta = 0$, in a 3 $\times$ 7 cluster equipped with GaAs or $\emptyset T$ preamps (cf. Fig.5 and Fig.6).*

Preamp	$\mathcal{L}$	$t_p^{opt}(\Delta)$	σ_{tot}	σ_{pu}	ENE_{tot}	ENE_F	ENE_{MB}
AsGa	10^{33}	62 ns	264 MeV	221 MeV	144 MeV	77 MeV	122 MeV
AsGa	10^{34}	37 ns	614 MeV	540 MeV	292 MeV	115 MeV	268 MeV
$\emptyset$T 25 Ω	10^{33}	72 ns	289 MeV	239 MeV	163 MeV	70 MeV	147 MeV
$\emptyset$T 25 Ω	10^{34}	43 ns	670 MeV	584 MeV	328 MeV	101 MeV	312 MeV

Table 5: *Optimum peaking time and noise values at $\eta = 1$, in a 3 $\times$ 7 cluster equipped with GaAs or $\emptyset T$ preamps (cf. Fig.7 and Fig.8).*

Preamp	$\mathcal{L}$	$t_p^{opt}(\Delta)$	σ_{tot}	σ_{pu}	ENE_{tot}	ENE_F	ENE_{MB}
GaAs	10^{34}	42 ns	435 MeV	374 MeV	223 MeV	116 MeV	191 MeV
$\emptyset$T 25 Ω	10^{34}	50 ns	472 MeV	408 MeV	237 MeV	101 MeV	215 MeV

Table 6: *Optimum peaking time and noise values at $\eta = 0$ in a 3 $\times$ 7 cluster with a 18 X_0 tapered Middle sampling (giving C_d = 1.5 nF) equipped with GaAs or $\emptyset T$ preamps (cf. Fig.10).*

Preamp	$\mathcal{L}$	$t_p^{opt}(\Delta)$	σ_{tot}	σ_{pu}	ENE_{tot}	ENE_F	ENE_{MB}
$\emptyset$T 50 Ω	10^{33}	37 ns	496 MeV	417 MeV	268 MeV	143 MeV	227 MeV
$\emptyset$T 50 Ω	10^{34}	30 ns	1244 MeV	1190 MeV	360 MeV	173 MeV	316 MeV

Table 7: *Optimum peaking time and noise values at $\eta = 2$ (End-Cap), in a 3 $\times$ 7 cluster equipped with $\emptyset T$ preamps (cf. Fig.9).*

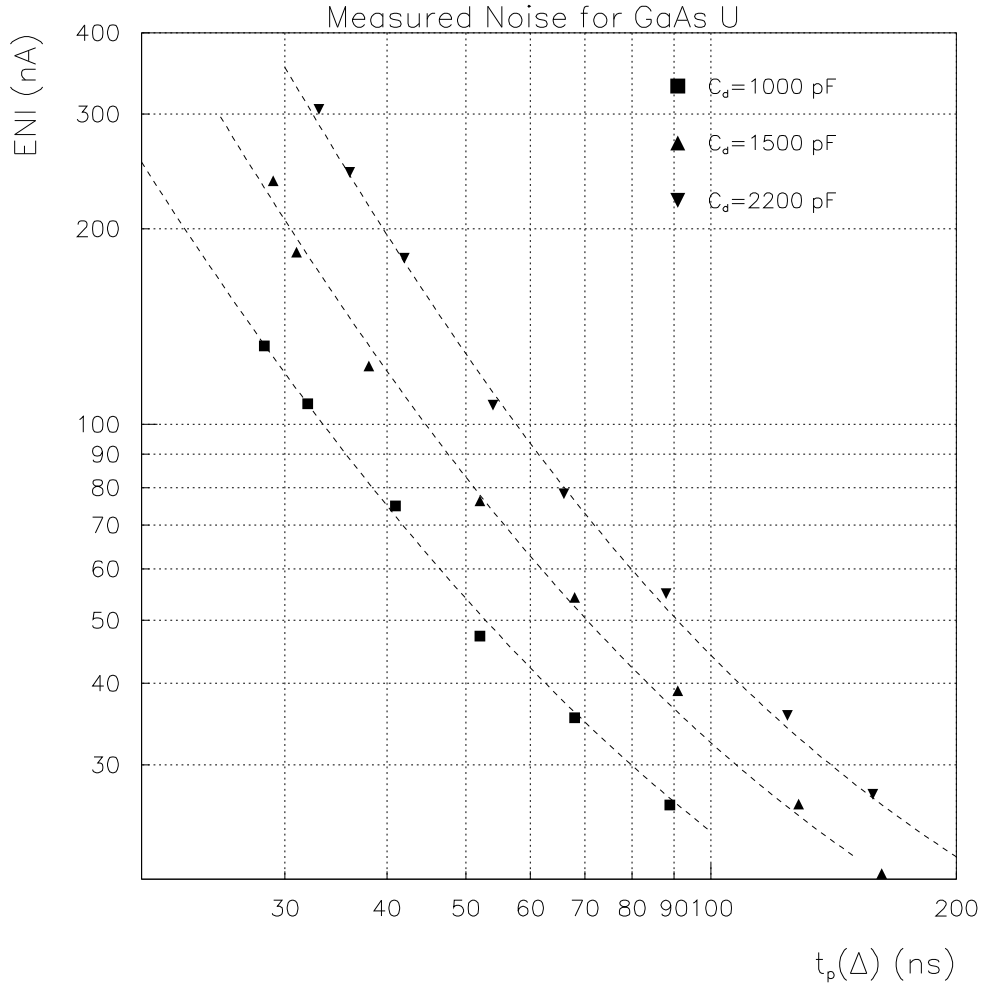

Figure 1: *Noise measurement [from N. Fedyakin] and fit of GaAs preamp in LAr, with C_d=1 nF, R_f = 800Ω, C_f = 22pF (bottom curve) and C_d= 2.2 nF, R_f = 400Ω (top curve). The fit coefficients A, B and C in Eq.(2) are given in Table 3. From Eq.(1), they correspond to e_n = 0.24 nV/$\sqrt{Hz}$ and i_n = 6.2 pA/$\sqrt{Hz}$. There was no high voltage protection and the shaper noise is quadratically substracted.*

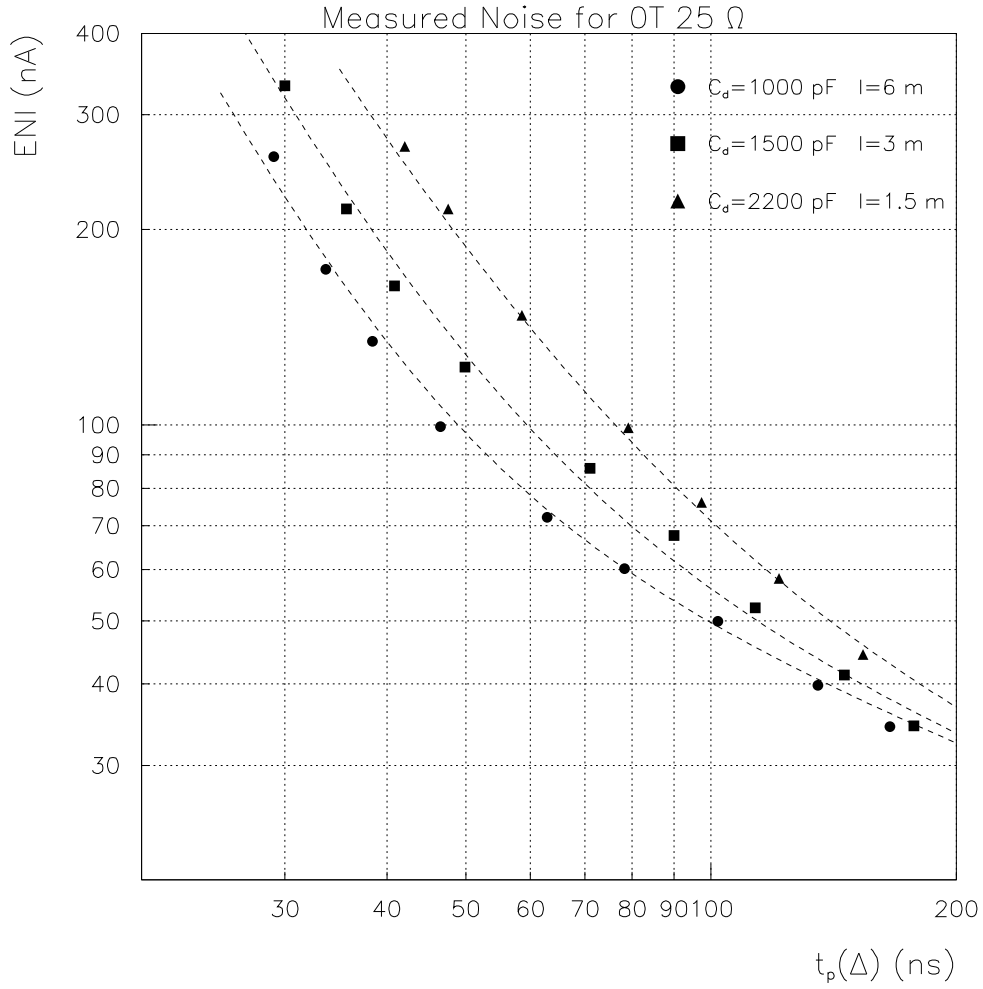

Figure 2: *Noise measurement and fit of ∅T preamp [from Y. Jacquier] with C_d = 1 nF, 6 meters 25 Ω cable (bottom curve) and C_d = 2.2 nF, 1 meter 25 Ω cable (top curve). The fit coefficients are given in Table 3. The cable used is two warm LEMO cables in parallel (cf. footnote 16) and the preamplifier settings are : $R_f = 750\Omega, R_1 = 1.5\Omega, R_2 = 51\Omega$ and I_c = 3.5 mA.*

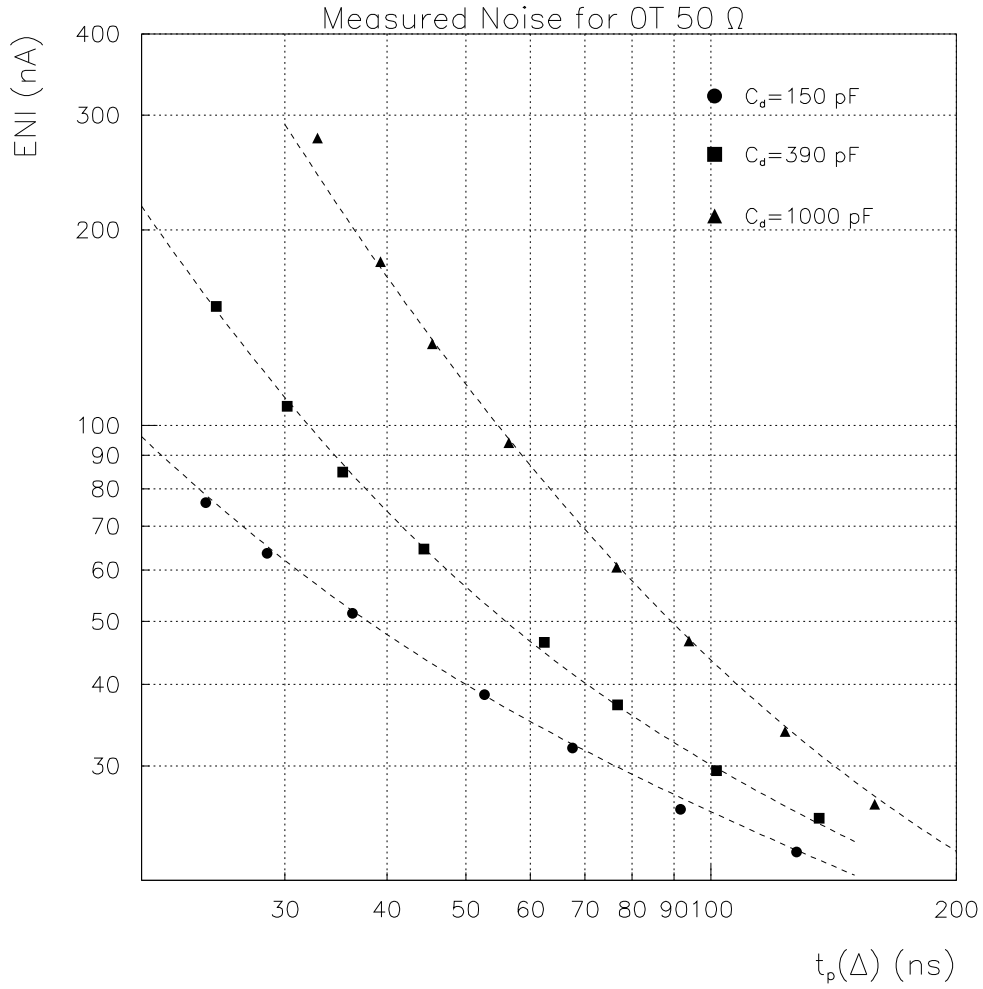

Figure 3: *Noise measurement and fit of ØT preamp with 6 meters 50 Ω cable for various detector capacitances. The cable used is a warm LEMO cable and the preamp settings are : $R_f = 1500\Omega, R_1 = 3.3\Omega, R_2 = 51\Omega$ and $I_c = 3.5$ mA (RD3 config.).*

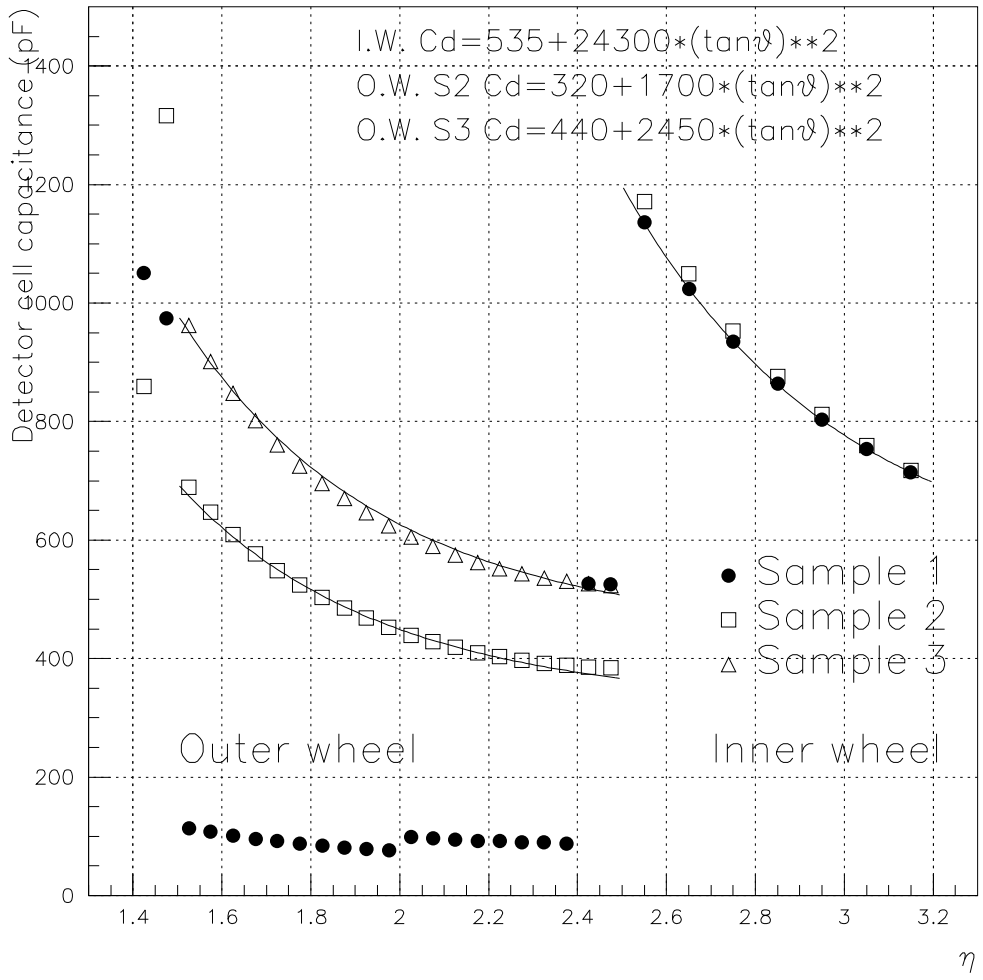

Figure 4: *Detector capacitance in the End-Cap and fit values [from O. Martin]*

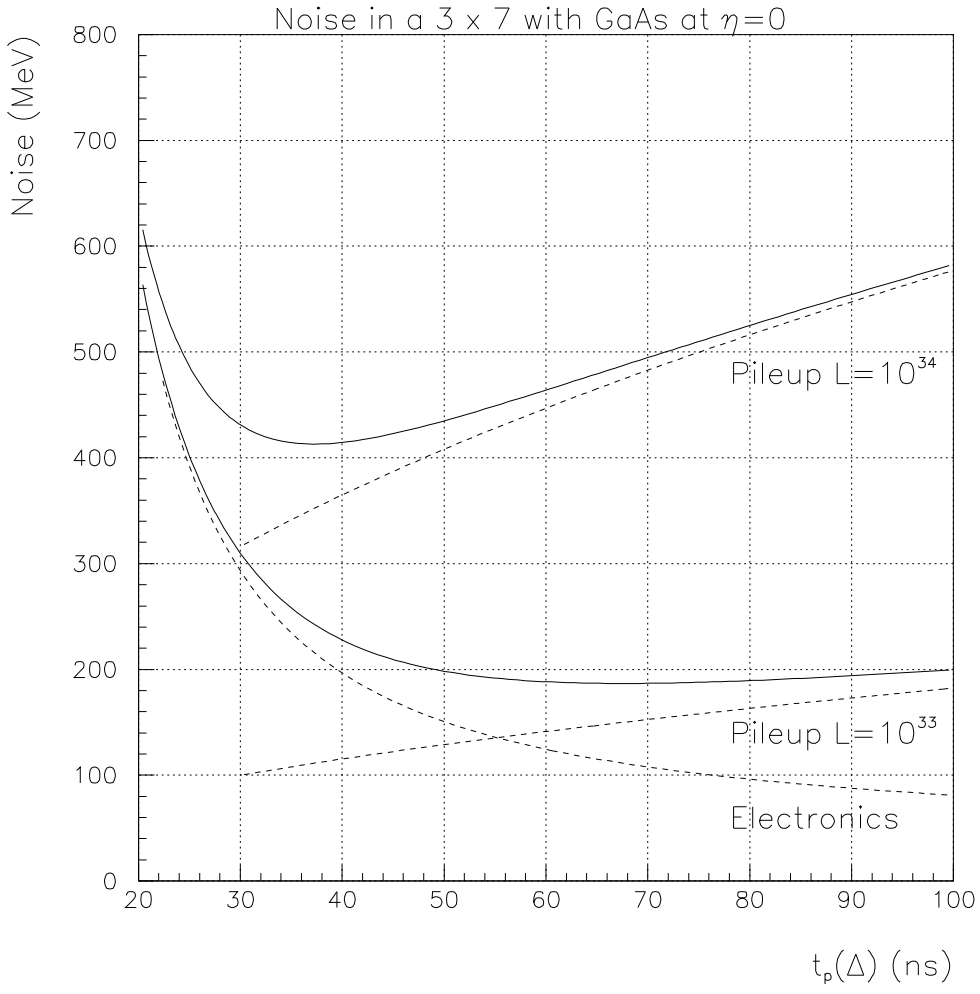

Figure 5: *Total noise with GaAs in a 3 × 7 cluster at $\eta = 0$. It is obtained by summing 48 cells in Front (equipped with $\emptyset T$ 50 Ω preamps) and 33 cells in Middle and Back equipped with GaAs preamps, using Eq.(6) and Eq.(10). The pileup is taken from Eq.(12).*

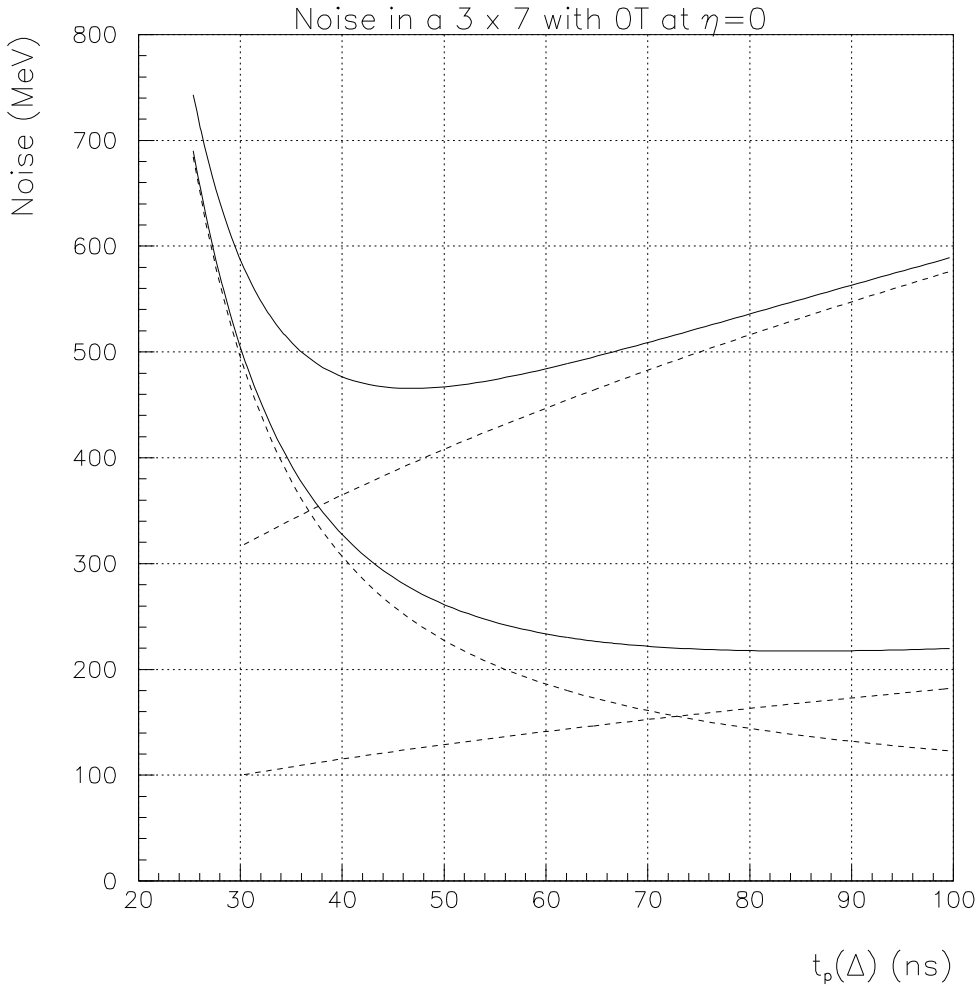

Figure 6: *Total noise with $\emptyset T$ in a 3 × 7 cluster at $\eta = 0$. It is obtained by summing 48 cells in Front (equipped with $\emptyset T$ 50 Ω preamps) and 33 cells in Middle and Back equipped with $\emptyset T$ 25 Ω preamps, using Eq.(6) and Eq.(11). The pileup is taken from Eq.(12).*

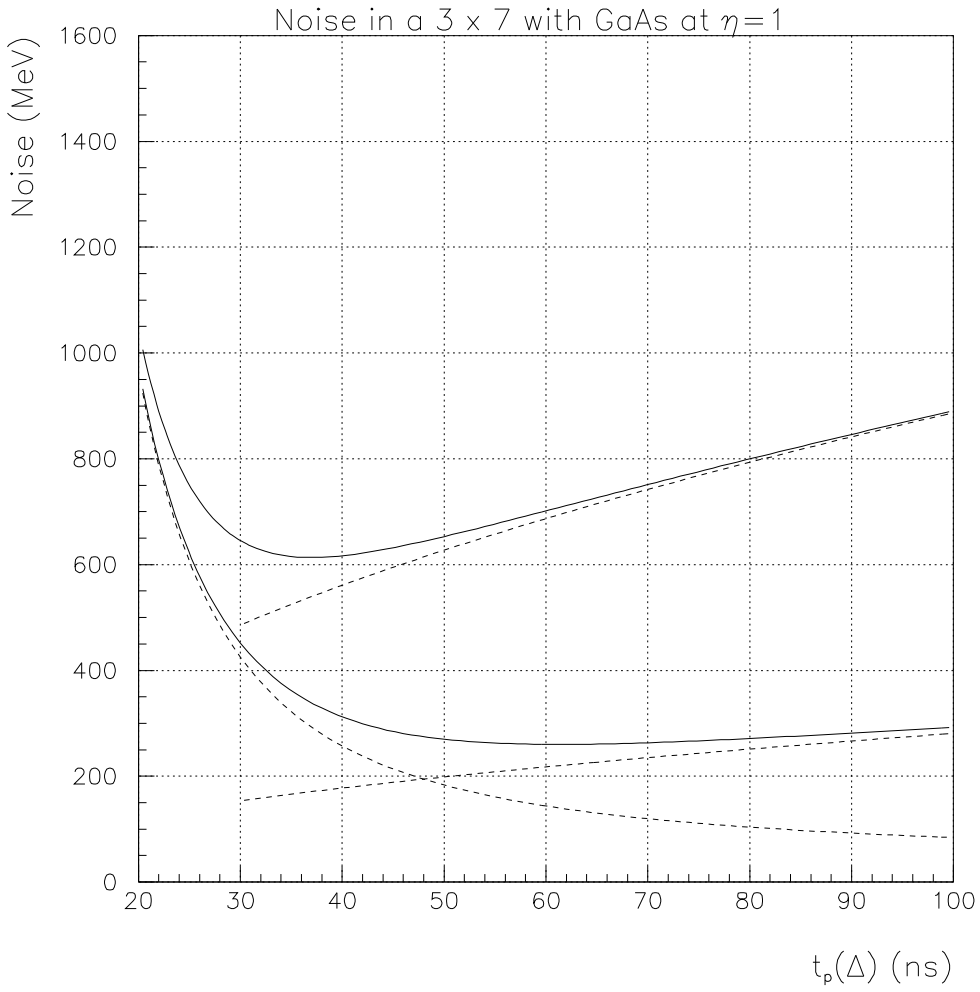

Figure 7: *Total noise with GaAs in a 3 × 7 cluster at* $\eta = 1$

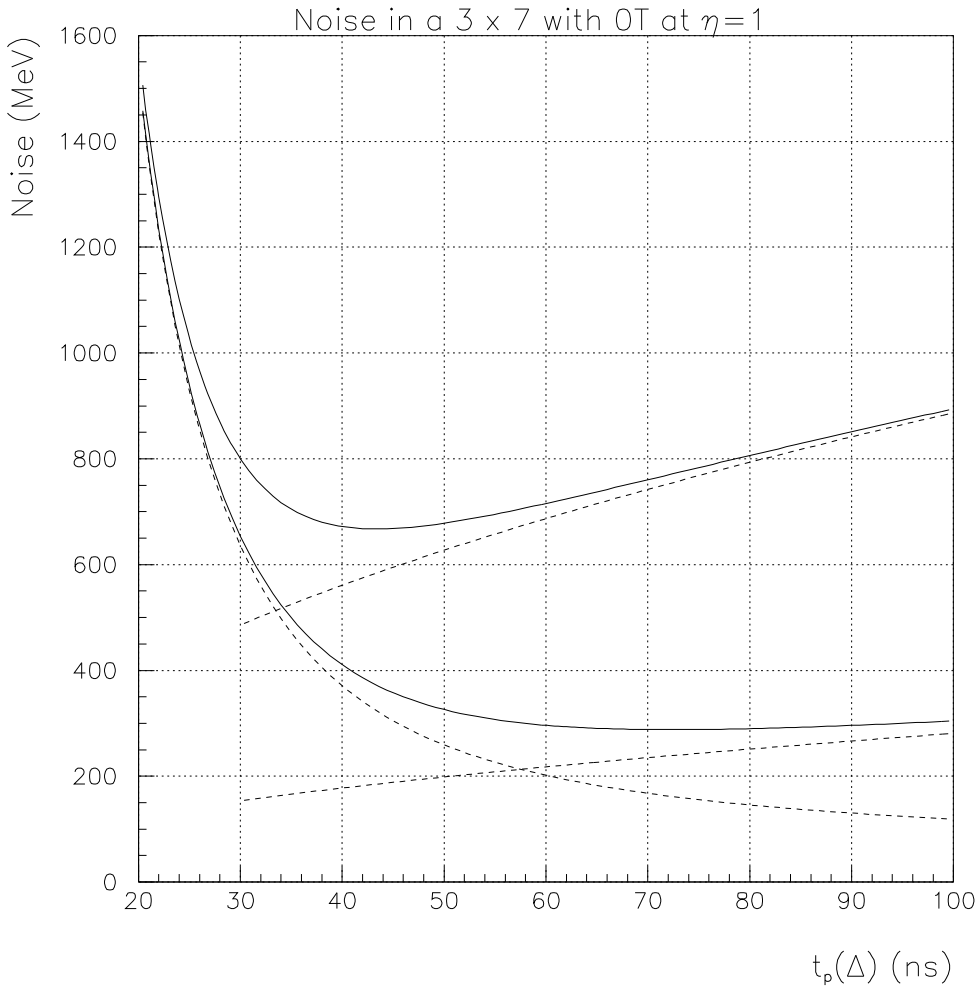

Figure 8: *Total noise with $\emptyset T$ in a 3 $\times$ 7 cluster at $\eta = 1$*

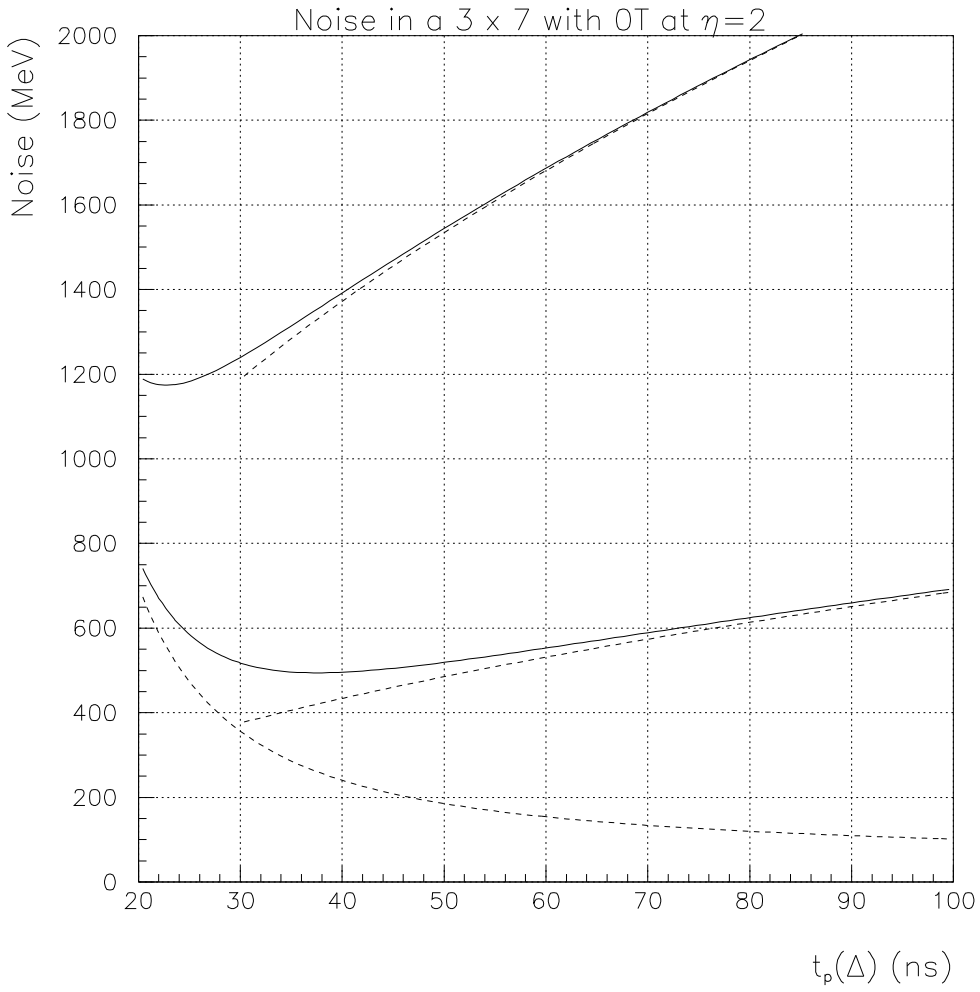

Figure 9: *Total noise with $\emptyset T$ 50 Ω in a 3 $\times$ 7 cluster in the End-Cap, at $\eta = 2$*

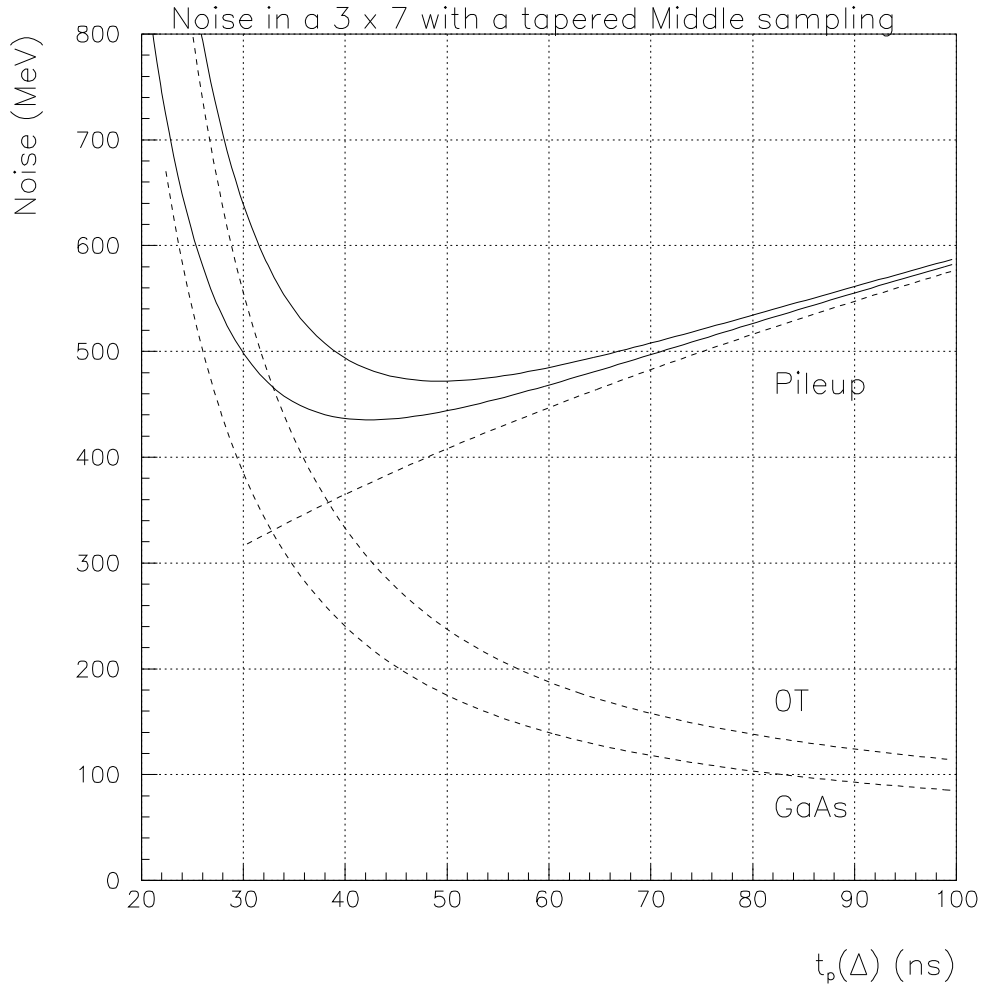

Figure 10: *Total noise at $\eta = 0$ in a 3×7 cluster with a Middle sampling tapered at 18 X_0, equipped with GaAs or $\emptyset T$. It is obtained by summing 48 cells in Front (equipped with $\emptyset T$ 50 Ω preamps) and 21 cells in Middle equipped with GaAs preamps or $\emptyset T$ 25 Ω using a detector capacitance C_d = 1.5 nF.*

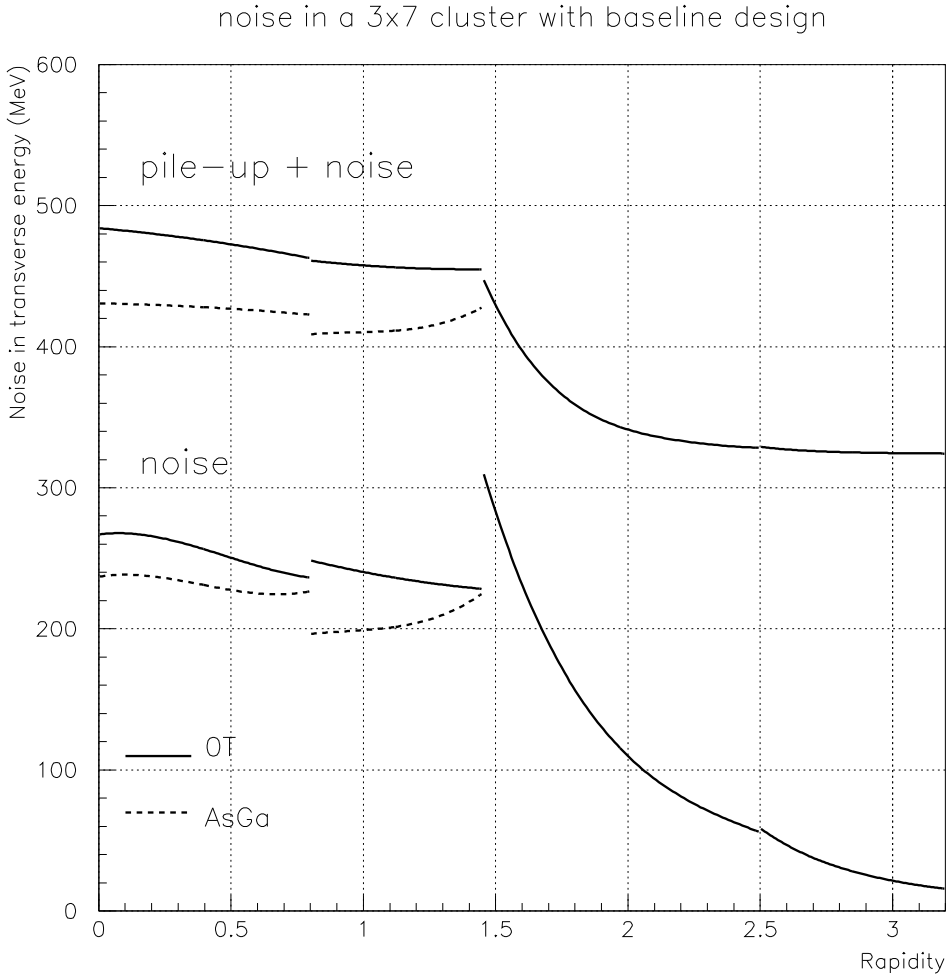

Figure 11: *Noise in transverse energy in a* 3×7 *cluster as a function of rapidity [from V. Tisserand]. The cluster size is* 1×2 *in the Presampler,* 24×2 *in the Front sampling equipped with* $\emptyset T$*,* 3×7 *and* 3×4 *for the Middle and Back samplings equipped with GaAs or* $\emptyset T$ *preamps in the Barrel. The shaping time is optimized in each region at the value given in Tables 4, 5 and 7 at* $\mathcal{L} = 10^{34}$*. The slight discrepancy in the noise values comes from the presampler and the calibration weights between samplings (15 for the Presampler, 1.123 for the strips and 1.05 for the Back at* $\eta = 0$*) used to optimize the energy resolution for 50 GeV* E_T *photons.*